Wetting properties of glycerol on mica and stainless steel by scanning polarization force microscopy

A. MOLDOVAN, M. BOTA, I. BOERASU, D. DOROBANTU, D. BOJIN, D. BUZATU, M. ENACHESCU[a,*]
Center for Surface Science and NanoTechnology, University "Politehnica" of Bucharest; Splaiul Independentei 313, Bucharest 060042, Romania
[a)]*Academy of Romanian Scientists, Splaiul Independentei 54, Bucharest 050094, Romania*

We studied the wetting properties of glycerol on mica and stainless steel (SS) using the Scanning Polarization Force Microscopy (SPFM) technique. The precise control of the polarization force between a conductive atomic force microscope tip and a substrate allowed topography profile measurements of micro- and nanodroplets of liquid, opening the opportunity for the determination of the interaction between the liquid and the substrate: contact angle and surface potential energy between the surfaces versus height of droplets. The results of these experiments offer insights into the mechanisms of wetting phenomena at liquid-solid interfaces, at the nanometer scale.

(Received March 20, 2013; accepted September 18, 2013)

Keywords: Scanning polarization force microscopy, Micro- and nanodroplets, Wetting, contact angle, Disjoining pressure

1. Introduction

The study of droplets or layers of liquid on top of solid surfaces has a great importance in quantifying the dispersion and wetting properties that appear at the gas/liquid, gas/solid and solid/liquid interfaces. The ability to visualize the 3D contour of the surface of liquid droplets or layers offers advantages in numerous applications (study of lubricants, surfactants, mechanisms and effects of corrosion, etc.) [1].

Atomic Force Microscopy (AFM) and related techniques of the Scanning Probe Microscopy (SPM) family allow the reconstruction of the 3D contour of the surfaces of solid materials with sub-nanometer lateral resolution and sub-Ångström vertical resolution. However, the magnitude of the forces that govern the tip-surface interaction in typical AFM experiments (either contact or intermittent contact) is high enough in most cases to disturb the liquid present at the surface [1,2].

Scanning Polarization Force Microscopy (SPFM) on the other hand uses electrostatic interaction (polarization) forces for topography feedback. As the range of the electrostatic forces is much longer compared to the range of the van der Waals forces (few nanometers), in SPFM the tip is able to scan the surface at larger separation from the surface. When a voltage is applied to the conductive AFM tip, the strong electrical field around its apex induces a polarization of the charge distribution on the nearby sample surface. The force can be detected at distances of a few tens of nanometers (i.e. 10–20 nm) from the surface and a constant force image can be obtained introducing it to the feedback control of the gap between the tip and the surface. Thus, SPFM allows the topographic imaging of soft surfaces and even liquid layers or droplets on any substrates, from conductors to thick insulators [2].

In order to analyze the shape and behavior of glycerol droplets we used the effect of long-range forces on the structure and wetting properties of liquids films, similar to the approach of de Gennes [3]. The shape $z(r)$ of a liquid drop on a solid surface can be obtained from minimization of the free energy G. For a circularly symmetric drop the free energy can be written as an integral over the area covered by the drop:

$$G = G_0 + \int_{\text{drop}} 2\pi r \, \mathrm{d}r \left[-S + \frac{\gamma}{2}\left(\frac{\mathrm{d}z}{\mathrm{d}r}\right)^2 + P(z) - \right.$$
$$\left. - \mu_{\text{vapor}} - \mu_{\text{liq}} \nu_{\text{mol}} \cdot z \right. . \quad (1)$$

The first term under the integral is $= \gamma_{\text{sv}} - \gamma_{\text{sl}} - \gamma$, the spreading coefficient; γ_{sv} is the solid-vapor surface energy; γ_{sl} is the solid-liquid surface energy; γ is the liquid-vapor surface energy. The second term is due to the excess surface because of the curvature of the drop and is valid for the case of shallow drops. The third term $P(z)$ is the surface potential energy between the surfaces, the energy needed to create a unit area of surface or interface. The last term describes the supersaturation in terms of chemical potentials of the vapor and liquid; ν_{mol} is the molecular volume of the liquid [3].

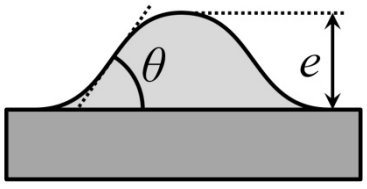

Fig. 1. Schematic drawing of the contact angle for the case of a microscopic droplet.

By minimization of G in eq.(1) under constant volume of droplet $V = \int z(r)\, 2\pi r\, \mathrm{d}r$ and assuming a spherical cap shape of the droplets [4], it gives for $z \to 0$ (near the base of the drop) that the relation between the effective contact angle θ (Fig. 1) and the disjoining pressure $\Pi(e) = -\frac{\mathrm{d}P}{\mathrm{d}e} = -P'(e)$ [5] is:

$$\theta^2 = \theta_0^2 + \frac{2}{\gamma}[P(e) + e\Pi(e)]\,, \tag{2}$$

where e is the height of the droplet, $\theta_0^2 = -\frac{2}{\gamma}P(0)$ is the macroscopic contact angle squared, $P(0)$ is the spreading coefficient S which characterizes the wetting properties of a surface by a given liquid at short ranges. If $S > 0$, the liquid will completely wet the surface and if $S < 0$, a contact angle will exist, determined by Young's equation: $\gamma \cos\theta = \gamma_{\mathrm{sv}} - \gamma_{\mathrm{sl}}$. The contact angle θ depends on the interfacial energies and is influenced by the disjoining pressure. The disjoining pressure is related to the spreading coefficient S by:

$$S = \int_0^\infty \Pi(x)\mathrm{d}x = P(e)_{e\to 0} \tag{3}$$

From eq.(2) it is obtained:

$$P(e) - eP'(e) = (\theta^2 - \theta_0^2)\frac{\gamma}{2} \tag{4}$$

Thus, the dependence of surface potential energy $P(e)$ between the surfaces can be determined after measuring experimentally the dependence of contact angle on droplet height in the case of spherical shaped droplets of small height.

2. Experimental studies of wetting phenomena

Apparatus description. The experiments were carried out in our laboratory using Scanning Polarization Force Microscopy (SPFM), a powerful technique for nondestructive imaging of liquid. The SPFM measurements were conducted in ambient air (room temperature, RH ~ 50%) using a modified home-built AFM controlled by commercial electronics (RHK SPM100 and PLLPro2). The samples were placed on steel carriers which were electrically connected to the ground of the system. SPFM measurements were carried out in AC mode, with a bias of 3V amplitude and 3kHz frequency applied between the conductive tip and ground. Commercial conductive coated (Pt and Cr/Au) contact mode silicon tips were used for the measurements (AppNano, Mikromasch, Nanosensors). The nominal spring constant of the cantilevers was less than 1 N/m.

Preparation of substrates. Glycerol was chosen for the formation of liquid droplets in these experiments and the substrates were mica and stainless steel.

Mica substrates were freshly cleaved prior to the experiments. Stainless steel substrates were polished using various grades of abrasive paper (gradually increasing the grit) and finally using slurry of alumina particles approximately 20 nm in size, dispersed on a felt disc. They were then sonicated for several cycles in methanol and deionized water for five minutes per cycle.

The substrates were verified by optical microscopy and AFM prior to the deposition of liquid droplets (Fig. 2 – optical microscopy images).

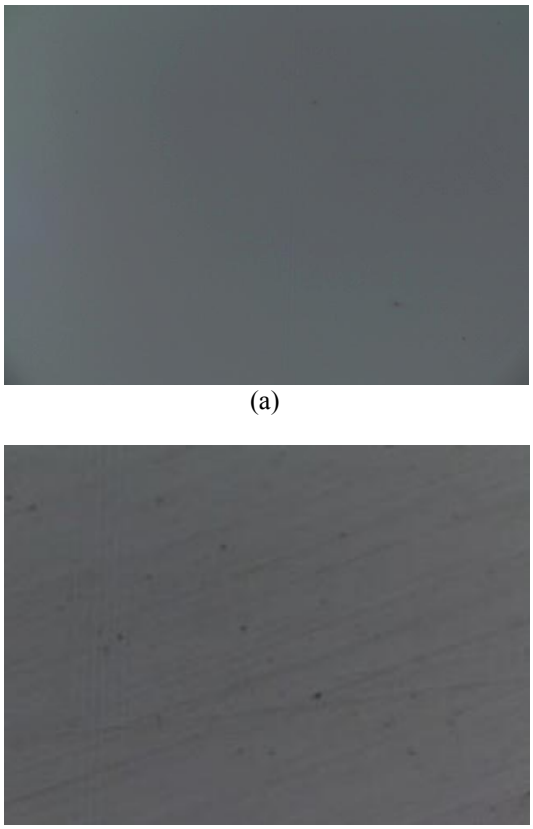

(a)

(b)

Fig. 2. Optical microscopy images of the substrates prior to the deposition of the droplets: a) mica; b) stainless steel; field of view ~80μm × 64μm.

Droplets deposition. Glycerol droplets were created on the substrates by condensation. The substrates were held upside down inside a Berzelius glass containing heated glycerol, at a height of ~1 cm from the liquid surface. After a few seconds the surface of the substrates achieved a "foggy" appearance, which proved the presence of microscopic droplets. This was confirmed by further optical microscopy inspection (Fig. 3).

(a)

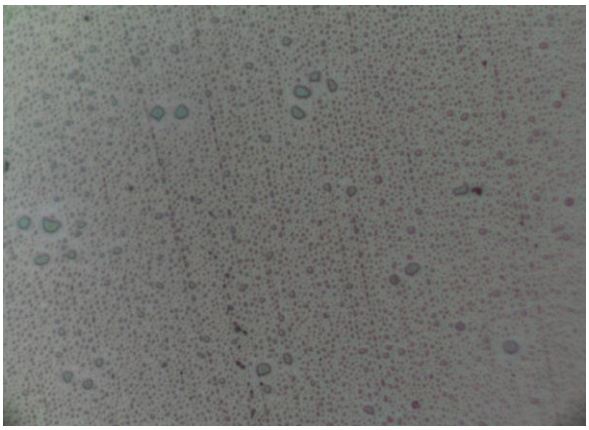

(b)

Fig. 3. Optical microscopy images of the substrates after the deposition of the droplets: a) glycerol on mica; b) glycerol on stainless steel. Field of view ~80 µm × 64 µm

3. Results and discussions

Optical microscopy. The image shown in Fig. 2a reveals a smooth surface of mica, almost free of any defect or impurity over large areas. In Fig. 2b, the surface of the stainless steel substrate shows some minor scratches which are due to the polishing process. The RMS roughness of the substrates assessed by AFM analysis (images not shown) was ~0.5nm for mica and ~30nm for stainless steel, on 30 µm × 30 µm areas.

Optical images shown in Fig. 3 are typical for the distribution of glycerol droplets on the substrates in these experiments. On mica glycerol tends to form many small droplets and few large droplets, while on stainless steel it only forms many small droplets. This could be attributed to the higher roughness of the steel surface, which prevents the droplets form migrating on the surface and merging into larger droplets.

SPFM analysis. Fig. 4 shows typical SPFM-AC topography images of the samples after the deposition of the droplets. These images confirm the general aspect of the droplets from the optical microscopy analysis.

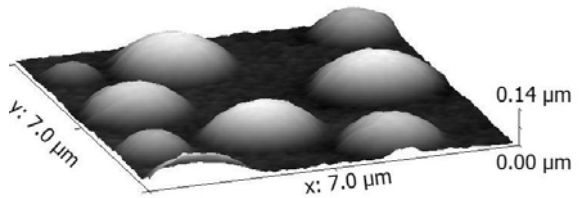

(a)

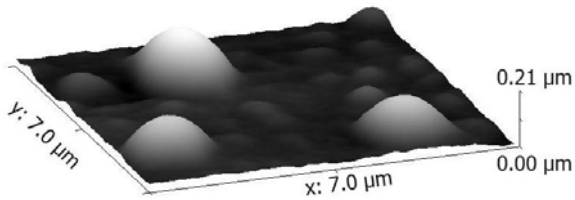

(b)

Fig. 4. Typical SPFM-AC images of the deposited droplets of glycerol on: a) mica b) stainless steel; field of view 7 µm × 7 µm.

Droplet profiles were extracted from the SPFM topography images of the samples, by plotting the height versus lateral displacement along horizontal segments taken across the point of maximum height for each chosen droplet. Some of the profiles are plotted in Fig. 5.

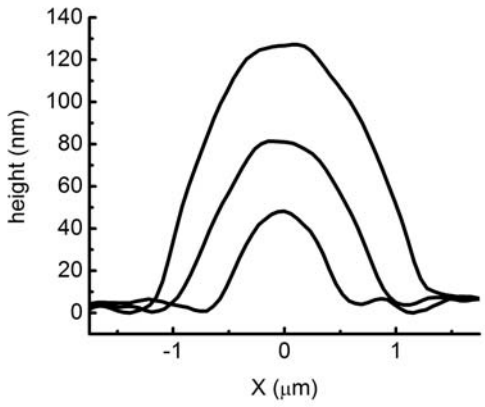

(a)

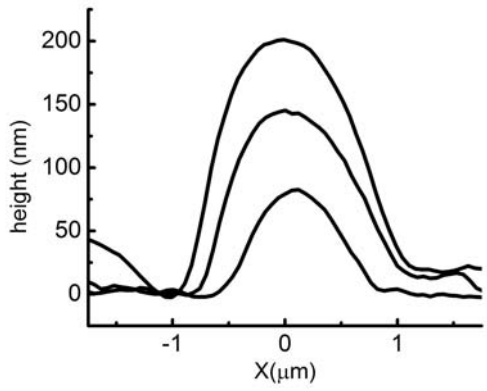

(b)

Fig. 5. Line-cut profiles of droplets of glycerol on: a) mica b) stainless steel

Contact angle measurements. For a macroscopic liquid droplet the contact angle is the angle at which the surface of the liquid meniscus meets the surface of the substrate, measured through the liquid. For micro- and nanodroplets, as shown in Fig. 5, the liquid meniscus does not meet the substrate surface at a precise angle and the graph of the line-cut profile has two inflection points, one on each side of the section (Fig. 1). In this case the microscopic contact angle is calculated by measuring the slope of the graph (first derivative) at these inflection points [1].

Contact angle values corresponding to the droplets shown in Fig. 4 were plotted as a function of droplet height (Fig. 6). A decrease of contact angle with droplet height is observed, which indicates that the surface potential $P(e)$ is negative, i.e. the interaction forces between surfaces are attractive or hydrophobic.

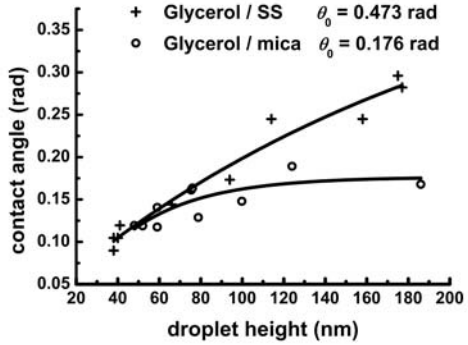

Fig. 6. Dependence of contact angle on droplet height for glycerol on mica and stainless steel.

The macroscopic contact angle θ_0 was determined as an exponential fitting parameter for the microscopic contact angle dependencies.

Potential energy measurements. Using relation (4) and the dependence of contact angle on droplet height (Figure 6) we calculate the dependence of surface potential energy $P(e)$ between the surfaces for glycerol on mica and stainless steel. The results are shown in Fig 7.

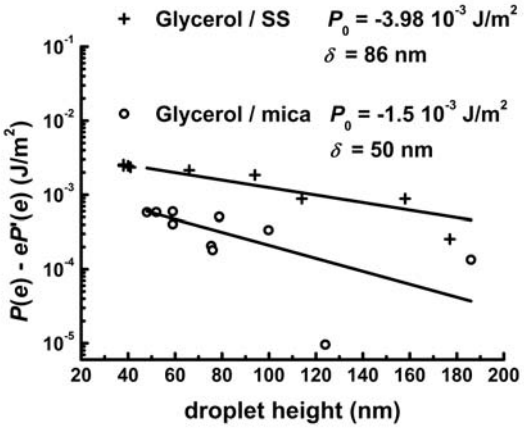

Fig. 7: Semilog plot of P(e)–eP'(e) vs. e, the droplet height, for glycerol on stainless steel and mica

On mica and stainless steel glycerol forms droplets whose shapes are close to spherical caps. The contact angle varies with height as shown in Fig. 6. The decrease of the contact angle with decreasing droplet height indicates that the surface potential $P(e)$ is negative and an exponential dependence $P(e) = P_0 \exp(-e/\delta)$ [4] with distance gives a good fit (Fig. 7), where P_0 and δ are the fitting parameters. From the fitting parameters we determine the dependence of the potential energy on droplet height:

$$P(e) = -1.4 \cdot 10^{-3} \exp(-e/50\ \text{nm})\ \text{J/m}^2 \text{ for glycerol on mica}$$

$$P(e) = -3.98 \cdot 10^{-3} \exp(-e/86\ \text{nm})\ \text{J/m}^2 \text{ for glycerol on stainless steel}$$

The exponential dependence of surface potential energy $P(e)$ with distance indicates hydrophobic attractive forces between the glycerol – mica/ stainless steel interfaces, having a decay length δ = 50 nm for glycerol on mica and δ = 86 nm for glycerol on stainless steel, values which dominate over the range of van der Waals forces. These forces may include double layer, solvation and hydration forces.

In our calculations we have used the value of 64 mJ/m^2 for the surface tension of glycerol.

The strength of the potential at e = 0 nm gives the spreading coefficient:

$$S = P(0) = -1.4 \cdot 10^{-3}\ \text{J/m}^2 \text{ for glycerol on mica}$$

$$S = P(0) = -3.98 \cdot 10^{-3}\ \text{J/m}^2 \text{ for glycerol on stainless steel.}$$

In both cases the values for spreading coefficient indicate a very weak hydrophobic interaction for these systems, by comparison with surface tension of glycerol. These potential energies give a negative disjoining pressure Π of 0.28 atm for glycerol on mica and 0.46 atm for glycerol on stainless steel. As we see, in the case of the glycerol on stainless steel the strength of the disjoining pressure appears to be two times higher than that for glycerol on mica system.

4. Conclusions

Wetting properties of glycerol on mica and stainless steel were studied at the nano-scale by a non-contact scanning probe technique. SPFM topographical images of glycerol droplets formed by condensation on the substrates were successfully recorded. This allowed us the direct determination of the microscopic contact angle. A decrease of microscopic contact angle with droplet height is observed, which indicates that the surface potential $P(e)$ is negative and has an exponential dependence. The dependence of surface potential energy $P(e)$ between the surfaces, the spreading coefficient (S < 0) and the disjoining pressure Π were calculated.

Acknowledgements

Financial support of the European Union and the Romanian Government, received through grants POSDRU/107/1.5/S/76813, POSCCE-O212-2009-2/12689/717, ERA-NET 4-001/07.04.2011, 13N11537–13N11538 and **IFA-CEA Nr. C2-08/01.03.2012** is gratefully acknowledged.

References

[1] M. Salmeron, Fundamentals of Tribology and Bridging the Gap Between the Macro- and Micro/Nanoscales, NATO Science Series Volume **10**, 651 (2001).
[2] J. Hu, X.-D. Xiao, M. Salmeron, Appl. Phys. Lett. 67 (1995)
[3] P.G. de Gennes, Rev.Mod.Phys. **57**, 827 (1985).
[4] L. Xu, M. Salmeron, J.Phys.Chem. B **102**, 7210 (1998)
[5] B.V. Derjaguin, N.V. Churaev, V.M. Muller, J.A. Kitchener, *Surface Forces* (chapter V), Consultants Bureau, New York, 1987

*Corresponding author: marius.enachescu@upb.ro